

Supporting Information

Polymer thin film adhesion utilizing the transition from surface wrinkling to delamination

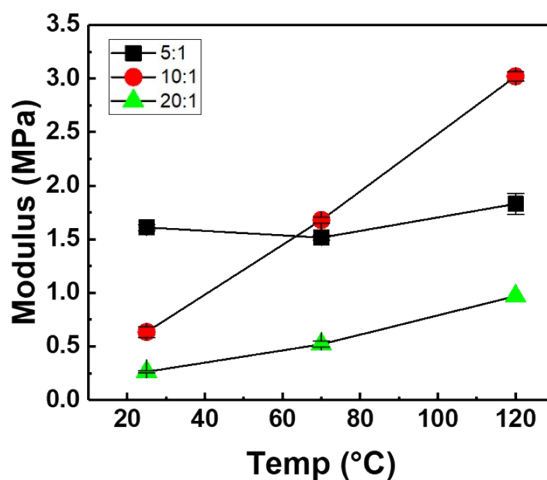
Hyeyoung Son, Allison L. Chau, Chelsea S. Davis*

School of Materials Engineering, Purdue University, West Lafayette, Indiana, 47906 USA

**Corresponding Author: Email address: chelsea@purdue.edu (C.S.D.)*

SI 1. PDMS Substrate Modulus Control

The Young's modulus of the poly(dimethyl siloxane)PDMS as the curing temperature and oligomer to crosslinker ration. PDMS which have 3 different mixing ratios, were cured at 25°C, 70°C and 120°C. To make fully cured PDMS, PDMS which is cured at 25°C, 70°C and 120°C were cured for 48hrs, 3hrs and 2hrs respectively. Fully cured PDMS was cut into 1mm by 3mm rectangular block to measure Young's modulus by using tensile testing (eXpert7603, ADMET). The results of Young's modulus of varied PDMS were shown in Figure S1. The Young's modulus of PDMS ranged from 0.26 to 3MPa. The error bars represent one standard deviation of at least 2 tests.



Ratio	5:1			10:1			20:1		
Temp (°C)	25	70	120	25	70	120	25	70	120
AVG (MPa)	1.61	1.52	1.83	0.64	1.68	3.02	0.26	0.52	0.97
STD(Mpa)	0.03	0.02	0.1	0.05	0.03	0.04	0.01	0.03	0

Figure S1. The Young's modulus of PDMS as the mixing ratio of oligomer to crosslinker and the curing temperature. The table shows exact value of Young's modulus and their standard deviations. The error bars represent one standard deviation of at least 2 tests.

SI 2. The film thickness as the concentration of PS and PMMA solution.

To control the film thickness for PS and PMMA, the concentration of PS and PMMA solution in toluene was varied from 1% to 5%. After coating the PS and PMMA film on Si wafer, the film thickness was measured by using interferometer (F20-UV thin film analyzer, Filmetrics). Figure S2 shows the variation of the film thickness as the polymer solution of PS and PMMA. PMMA is slightly lower than PS film with same concentration, the relationship between the film thickness and the concentration of solution was linear. The error bars were in the symbol, and they represent one standard deviation of 3 tests.

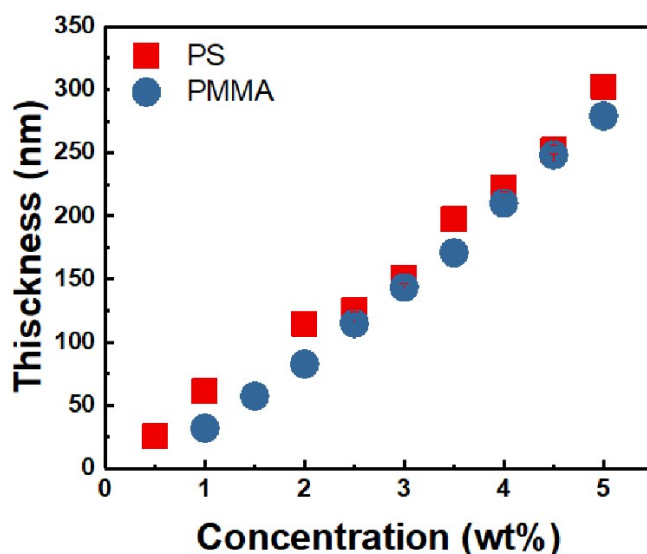


Figure S2. The variation of the film thickness as the polymer solution of PS and PMMA. The error bars show the one deviation of at least 3 tests and are smaller than the data points in most instances.

SI 3. The custom-built cutting system

Figure S3 shows the custom-built cutting system. The manual stage which could move in x-direction was built to optical support rod, then the razor blade was fixed above the manual stage. The silicon wafer was placed on the manual stage with double sided adhesive tape to fix the wafer.

The tip of the razor blade was placed on the film surface, then stage moved in uniaxial direction. As a result, the film was cut in linear line. As attaching the ruler tape on the stage, the film cut with 1mm by 5mm size.

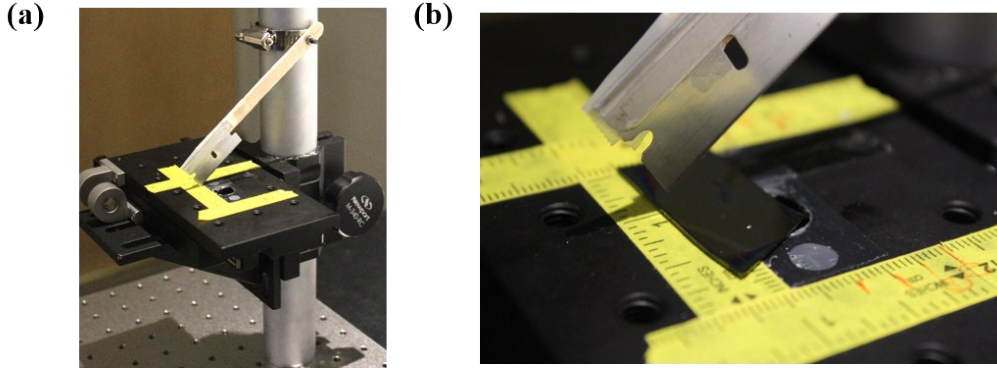


Figure S3. The picture of custom-built cutting system (a) and the stage image with the sample.

SI 4. The effect of residual stress on film buckling

Experiments were performed to determine the impact of residual stress in the glassy PS and PMMA films on their out-of-plane buckling behavior. Wrinkle amplitude for a stress-free film is

given by $A = t \sqrt{\frac{\varepsilon}{\varepsilon_w} - 1}$ where t is film thickness, ε is applied strain, and ε_w is critical strain for wrinkling. Here, the predicted value for ε_w was calculated from measured materials properties

using the critical strain for wrinkling relationship: $\varepsilon_w = \frac{1}{4} \left(\frac{3E_s}{E_f} \right)^{\frac{2}{3}}$. With these relationships, the predicted, stress-free wrinkle amplitude can be calculated. It has been reported previously that significant residual stress in a glassy film can result in suppression of the wrinkle amplitude for a given strain (ACSnano, 2009,3,844-852). By comparing measured amplitudes with the predicted values, the impact of residual stress can be observed in a straightforward manner.

Next, the wrinkle amplitude was measured as the lateral compressive strain was gradually increased for our materials system. Wrinkle amplitude was measured using an optical profilometer

(Zygo NewView 8300). Samples of PS and PMMA ($t=167$ nm for PS, $t=146$ nm for PMMA) and PDMS ($\bar{E}_s=1.23$ MPa) were studied. The strain on the sample was increased in steps of $\sim 0.3\%$. Fig S4 shows the measured wrinkle amplitude as a function of applied strain with the solid lines in the graph illustrating the predicted “stress-free” amplitudes. It can be seen that there is very little difference between the predicted wrinkle amplitudes and the measured values. Therefore, residual stress effects were not observed to significantly impact the wrinkle amplitude, and are therefore assumed to be negligible for this W2D work.

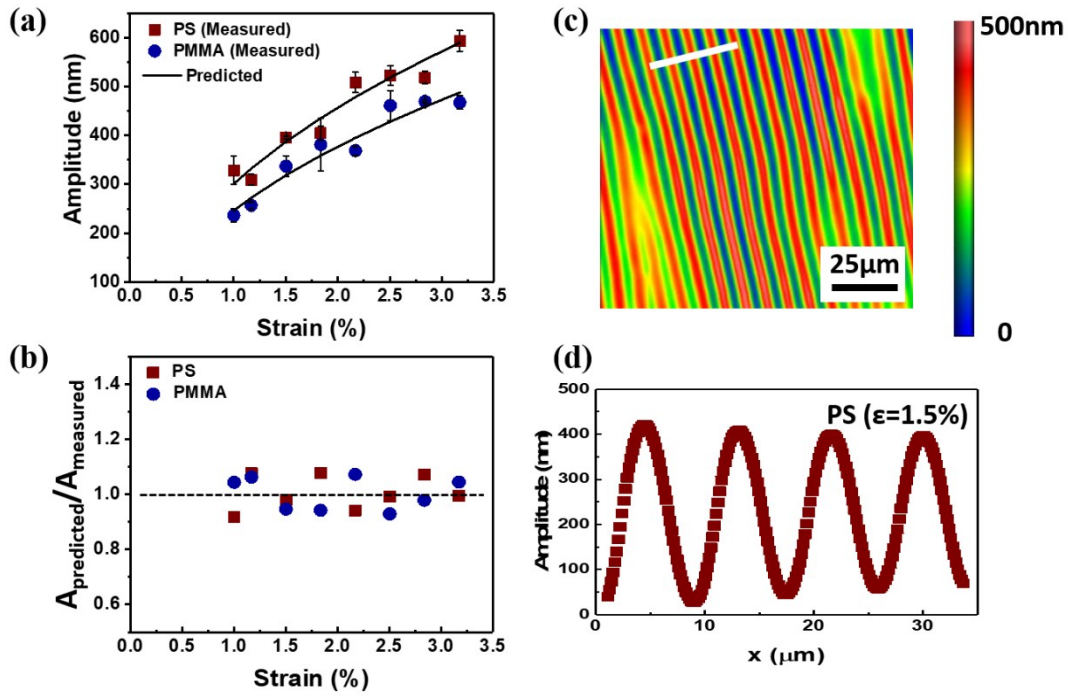


Figure S4. The effect of residual stress on wrinkle amplitude for PS and PMMA ($t=167$ nm for PS, $t=146$ nm for PMMA) and PDMS substrate moduli ($\bar{E}_s=1.23$ MPa) (a) The predicted and measured wrinkle amplitude was nearly identical over a range of strains. The error bars represent one standard deviation of at least 3 regions of interest. (b) The ratio of predicted amplitude over measured amplitude. (c) Optical profilometry scan of PS at $\epsilon=1.5\%$. The white line in (c) indicates the location of the scan for the data shown in (d). (d) Height profile of wrinkles.

SI 5. The plane strain modulus of PS and PMMA film by thickness measured by wrinkle wavelength method

The plane strain modulus (\bar{E}_f) of PS and PMMA film was measured using the wavelength of wrinkles which are observed during each W2D test. Using image analysis software (ImageJ, NIH), each wrinkle image was analyzed. Figure S5 shows \bar{E}_f of PS and PMMA film with film thickness. Each data point is calculated based on eqn (1) and is determined using experimentally measured \bar{E}_s and t values. The average \bar{E}_f for PS and PMMA was $4.0 \pm 1.3 \text{ GPa}$ and $3.5 \pm 0.5 \text{ GPa}$, respectively. The large amount of variation is likely due to the propagation and amplification of error in the measurement of substrate modulus, film thickness, and wrinkle wavelength. It can be seen from both plots that \bar{E}_f was consistent over the range of film thicknesses used in this study.

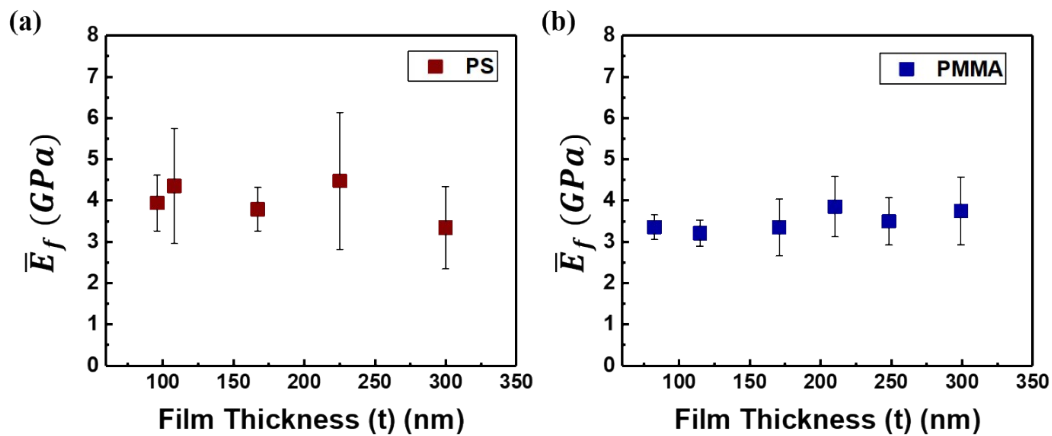


Figure S5. The plane strain moduli of PS (a) and PMMA (b) as a function of film thickness.

SI 6. W2D evolution of film surface with increasing strain

These two videos show the change in the morphology of PS films (ESI Video 1: $t=110\text{nm}$ and ESI Video 2: $t=350\text{nm}$) on PDMS ($\bar{E}_s=0.36\text{MPa}$) as the strain is increased. In the bottom left corner of the video, the strain value is given for each strain step/frame. The critical strain of delamination

for these film-substrate systems were 4.5% for the thinner film and 1.9% for the thicker film, at which point delaminations initiate and continue to propagate, though no additional strain is added to the system beyond the critical point.